Aligned Sub-10-nm Block Copolymer Patterns

Templated by Post Arrays

Jae-Byum Chang[†‡], Jeong Gon Son[†‡], Adam F. Hannon[†], Alfredo Alexander-Katz[†], Caroline A. Ross[†], and Karl K. Berggren*[,§]

[†]Department of Materials Science and Engineering and [§]Department of Electrical Engineering and Computer Science, Massachusetts Institute of Technology, Cambridge, Massachusetts, 02139. [‡]These authors contributed equally to this work.

E-mail should be addressed to: berggren@mit.edu

Abstract

Self-assembly of block copolymer films can generate useful periodic nanopatterns, but the self-assembly needs to be templated to impose long-range order and to control pattern registration with other substrate features. We demonstrate here the fabrication of aligned sub-10-nm linewidth patterns with a controlled orientation by using lithographically-formed post arrays as templates for a 16 kg/mol poly(styrene-block-dimethylsiloxane) (PS-*b*-PDMS) diblock copolymer. The in-plane orientation of the block copolymer cylinders was controlled by varying the spacing and geometry of the posts, and the results were modeled using 3D self-consistent field theory. This work illustrates how arrays of narrow lines with specific in-plane orientation can be produced, and how the post height and diameter affect the self-assembly.

Self-assembly of block copolymers is currently of interest as a method for fabricating nanopatterns.[1-4] It can generate dense arrays of nanoscale spherical, cylindrical or lamellar microdomains which can be used as lithographic masks.[5-7] Compared with conventional lithography methods, the self-assembly of block copolymers has two advantages: (1) the periodicity of dense structures can be scaled down to ~10 nm, which is well beyond the resolution limit of optical lithography;[8] and (2) nanopatterns can be fabricated over a large area in parallel, so the throughput can be several orders of magnitude higher than that of electron-beam lithography (EBL).[9] Based on these two advantages, self-assembly of block copolymers has been used in the fabrication of devices including nanocrystal flash memory, nanowire transistors, gas sensors, patterned magnetic recording media, and contact holes for transistors.[10-15]

Microdomains generated in a self-assembled block copolymer film can be guided by templates to produce nanopatterns with a precisely determined orientation and long-range order. Periodic templates, such as chemical patterns,[16-20] topographic trenches,[21-22] facets of single crystal sapphire,[23] or other block copolymers[8, 9] have been used to impose long-range order on the microdomains. In prior work, sparse post arrays were used to control the in-plane orientation of 51 kg/mol spherical and 45.5 kg/mol cylindrical morphology poly(styrene-*block*-dimethylsiloxane) (PS-*b*-PDMS) block copolymer microdomains with a period of 40 nm and 34 nm respectively.[24,25] Designed post arrays were also used to locally control the orientations of the cylindrical microdomains, and to generate complex device-like nanopatterns.[25]

To achieve sub-10-nm complex nanopatterns based on the self-assembly of block copolymers, a block copolymer with a sub-10-nm periodicity and a process for templating its self-assembly are required. Sub-10-nm periodicity has been achieved by various block copolymer systems, such as PS-*b*-PDMS,[8,9] PS-*b*-PEO,[23,27] and PMMA-*b*-PMAPOSS.[26] Several different approaches

4

have been used to template the self-assembly of a block copolymer with a sub-10-nm periodicity, but sub-10-nm block copolymer patterns with a specific registration with substrate features have not yet been demonstrated.[8,9,23,28]

In this article, we present a method for achieving well-oriented and registered sub-10-nm PS-*b*-PDMS block copolymer patterns using topographic templates. To template the self-assmebly of PS-*b*-PDMS with a sub-10-nm periodicity, the diameter of the posts must also be scaled down to the sub-10-nm range in concert with using lower molecular weight block copolymers which generate periodic patterns with sub-10-nm features. However, the fabrication of sub-10-nm posts is challenging even with state-of-the-art lithography.[30] To overcome this challenge, processes are needed to fabricate the templates, and a better understanding of the interaction between the microdomains and the posts is required. In this work, the templated self-assembly of a 16 kg/mol cylindrical morphology PS-*b*-PDMS block copolymer with 18 nm period is demonstrated using sparse topographic templates. The interaction between the block copolymer and post templates with a range of diameters and heights was examined, and topographic templates were designed to align the block copolymer microdomains in specific directions on the substrate.

RESULTS AND DISCUSSION

A 16 kg/mol cylindrical morphology PS-*b*-PDMS block copolymer (PDI ~1.08, f_{PS} ~0.69) was spin-coated onto a substrate to form a monolayer of in-plane PDMS cylinders. The thickness of the film was 24 nm, which is commensurate with a 18-nm-periodicity in-plane cylinder, a top surface layer of PDMS, and a bottom surface layer of PDMS. A 24-nm-thick films of the block copolymer were annealed in an acetone vapor in a chamber with a small leak until complete evaporation of solvent (~ 4 hr). During the solvent annealing, each block swelled to a different

swelling ratio (PS ~ 1.62, PDMS ~ 1.44), which increased the effective f_{PS} from 0.67 to 0.70[28].

Solvent uptake by the film lowered the Flory-Huggins interaction parameter compared to that of

the dried film.[29] The annealed films were etched by oxygen plasma to remove the PS and reveal

the oxidized PDMS microdomains. Figure 1(a) shows randomly oriented linear patterns with 18

nm periodicity formed on a smooth substrate.

To impose long-range order and to control pattern registration, we used rectangular arrays of

posts with various periods L_x and L_y, as depicted in figure 1(b). In prior work, posts with heights

of ~35 nm and diameters of ~10 nm were effective in templating the self-assembly of a 45

kg/mol cylindrical morphology PS-b-PDMS block copolymer with periodicity of 34 nm.[25]

Extrapolation of these dimensions suggests that posts with a height of ~18 nm and a diameter of

~5 nm would be needed to effectively template the self-assembly of a 18 nm period block

copolymer. However, fabricating posts with diameter smaller than 10 nm is difficult with a

conventional electron beam lithography system.[30] In this work, posts were fabricated with

diameters of 6.3 nm – 13.8 nm and heights of 12 – 27 nm from high-contrast negative-tone-resist

hydrogen silsesquioxane (HSQ) and a high contrast salty development system.[30]

The posts were functionalized with a PDMS brush to be attractive to the PDMS block of the

block copolymer. Prior work on a 34 nm period block copolymer[25] showed that the cylindrical

PDMS microdomains contact the PDMS-coated posts and orient in plane so as to minimize the

strain in the microdomain lattice, i.e. the commensurability between the post lattice and the

equilibrium period L_o governs the self-assembly. For example, if $L_o = nL_x$ (with n an integer) then

the microdomain lattice is commensurate with the L_x spacing and the cylinders are expected to

orient along the y-axis with zero strain.

Fig. 1(c-t) shows templating using posts with a height of 19 nm and a diameter of 10 nm. By varying L_x from 29 nm to 72 nm with L_x/L_y = 1.15 and 1.5, we demonstrated every possible commensurate condition for the 18 nm period PS-*b*-PDMS, in which the orientation of the block copolymer cylinders could be varied between 0° and 90° with respect to the *x*-axis. The block copolymer cylinders formed an aligned linear pattern when the post arrays satisfied one of the commensurate conditions, exactly analogously to the case of the 34 nm period block copolymer[25]. This result shows that an aligned linear pattern can be achieved by topographic post templates even for microdomains in the sub-10 nm regime. The final pattern achieved by topographic templates and a block copolymer can then be transferred into metal using previously demonstrated techniques[9].

To minimize the time required for template fabrication, it is desirable for the posts to be as sparse as possible. Fig. 1(k) shows good order even when the posts only occupy 5% of the final PDMS pattern, suggesting that this method of templated self-assembly can be considered as a method to increase the throughput of EBL by a factor of ~20. To decrease the density of the templates further, the posts can be replaced by well-spaced 'dashes' or fins which provide additional guidance to determine the in-plane orientation of the cylinders. Those results are given in the Supporting Information, which shows long-range ordered sub-10-nm block copolymer patterns guided by dash templates which occupied only 1/66 of the final pattern.
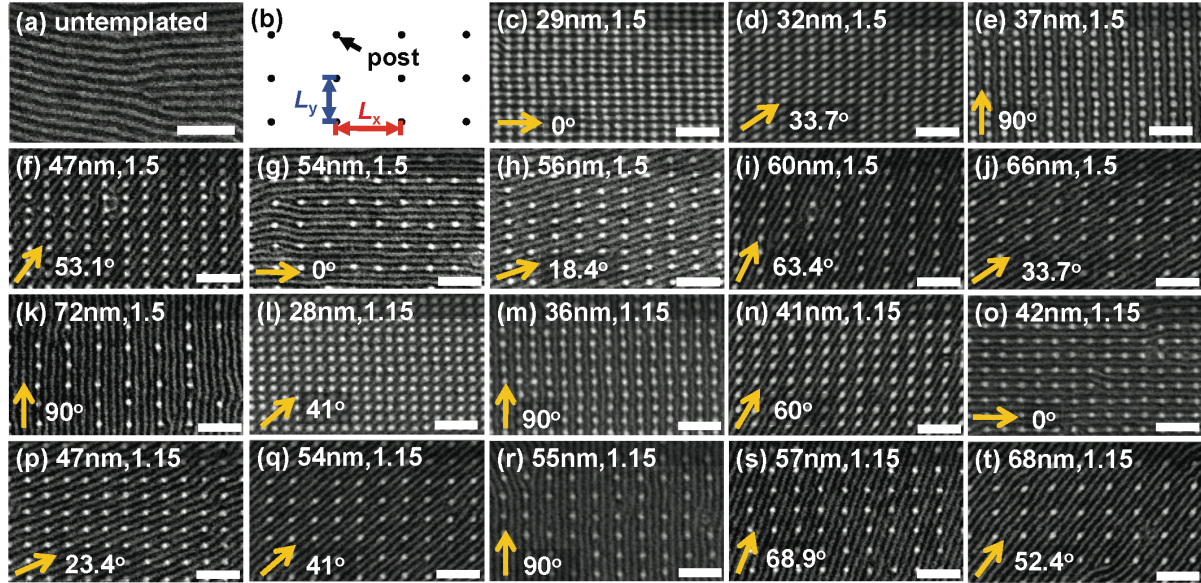
Figure 1. (a) SEM image of PDMS microdomains on a smooth substrate; (b) The definition of L_x and L_y of the post arrays; (c~t) SEM images of PDMS cylinders templated by post arrays. The height of the posts was 19 nm and the diameter was 10 nm. Arrows indicate the direction of the PDMS cylinders. Each figure is annotated L_x, L_x/L_y. (c~k) $L_x/L_y = 1.5$ (l~t) $L_x/L_y = 1.15$. Scale bar = 100 nm.

We now consider the effects of post height and diameter on the templating process. Figure 2 illustrates how a block copolymer interacts with posts with a range of diameters, for $L_x = 48$ nm and $L_y = 32$ nm and a post height of 16 nm. The commensurate orientation of the 16 kg/mol PS-b-PDMS block copolymer cylinders for this array period is depicted in figure 2(a), giving a cylinder orientation of 53.1° with respect to the x-axis. At a height of 16 nm, posts with diameter ranging from 6.3 nm to 13.8 nm could be obtained; posts fell over when the aspect ratio was larger than ~3. Figure 2(b~g) shows the PDMS cylinders templated by posts with a range of diameters. As shown in figure 2(b), the PDMS cylinders were not aligned in a preferential

orientation when templated by posts with a diameter of 6.3 nm, which is smaller than the width of the PDMS microdomain. However, the PDMS cylinders were aligned along the commensurate orientation (53.1°), when templated by posts with diameters comparable to the width of the PDMS microdomain, as shown in figure 2(c~f), although the PDMS cylinders lost long-range order and some fractions were aligned parallel to the y-axis, as shown in figure 2(g).

Figure 2(h) shows how the orientation of the block copolymer cylinders depended on the post diameter for a given post spacing. The distribution of cylinder orientations was found by a MATLAB image analysis program, which determined the area fractions of cylinders oriented parallel to the y-axis (90°) and along the 53.1° commensurate orientation. The cylinders formed the expected commensurate orientation over >80% of the post lattice when the post diameter was in the range from 8 nm to 12 nm, which is comparable to the width of the PDMS microdomains. The maximum area fraction was achieved with a post diameter of 11 nm.
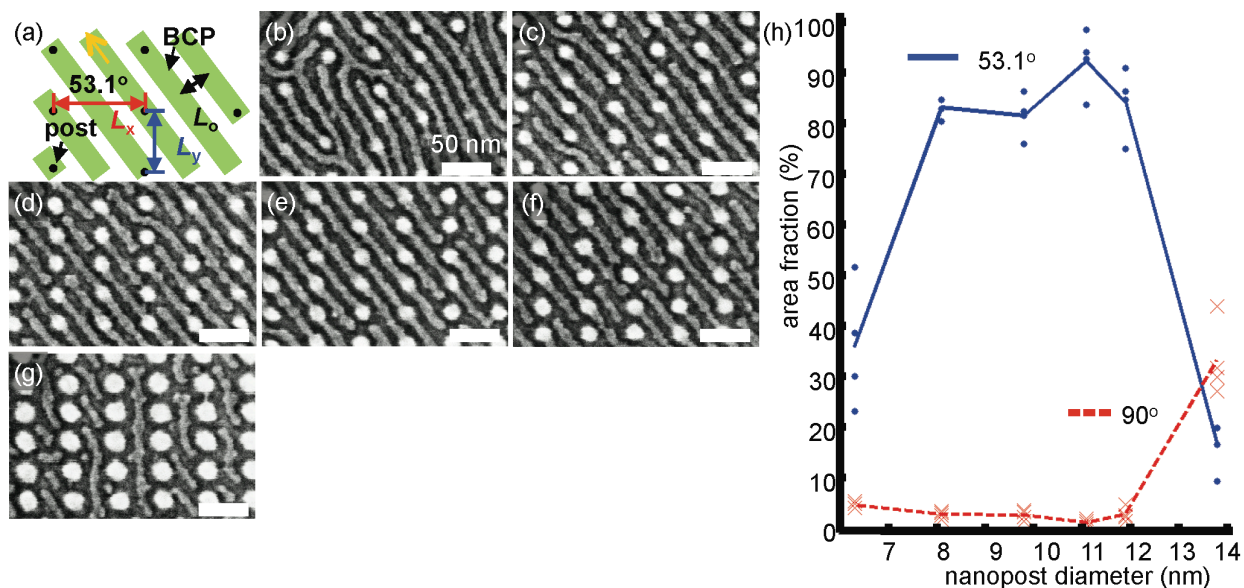

Figure 2. (a) The commensurate orientation for a post array with L_x = 48 nm and L_y = 32 nm. (b~g) PDMS microdomains templated by arrays with various post diameters with L_x = 48 nm and L_y = 32 nm and a post height of 16 nm. The diameter of posts was (b) 6.3 nm (c) 8.1 nm (d) 9.8

9

nm (e) 11.1 nm (f) 11.9 nm (g) 13.8 nm. Scale bar = 50 nm. (h) the area fraction of the cylinders oriented along the commensurate orientation and the fraction along the y-axis. (b~g) the samples were slightly overetched, which makes the PDMS cylinders disconnected.

When the post diameter was larger than 12 nm, the area fraction of the block copolymer cylinders oriented along the commensurate orientation decreased and the cylinders broke into shorter segments. Instead of aligning along the commensurate orientation, the block copolymer cylinders often lay along the larger gaps between the posts, parallel to the y-axis. The 12 nm diameter posts are wider than the equilibrium width of the cylindrical microdomain, leading to considerable distortion of the PDMS chains in the microdomain surrounding the post, which destabilizes the commensurate condition. Further information about how the orientation of PDMS cylinders changed depending on the post diameter is included in the Supporting Information.

Figure 3 shows how the block copolymer interacted with posts with a range of heights, 12 nm to 27 nm. The arrays had L_x of 48 nm and L_y of 32 nm, and a post diameter of 12 nm. The PDMS cylinders were not aligned when templated by posts with a height of 12 nm, as shown in figure 3(a). However, the PDMS cylinders were aligned and oriented along the commensurate orientation when templated by posts with a height of 16 nm, which is comparable to the equilibrium period of 16kg/mol PS-b-PDMS, as shown in figure 3(b). Figure 3(c~e) shows that the PDMS cylinders were oriented parallel to the y-axis when templated by posts taller than 19 nm. The area fractions in figure 3(f) were consistent with the above observations. A post height of 16 nm gave the highest fraction of the commensurate orientation, while taller posts promoted a y-axis orientation of the cylinders.
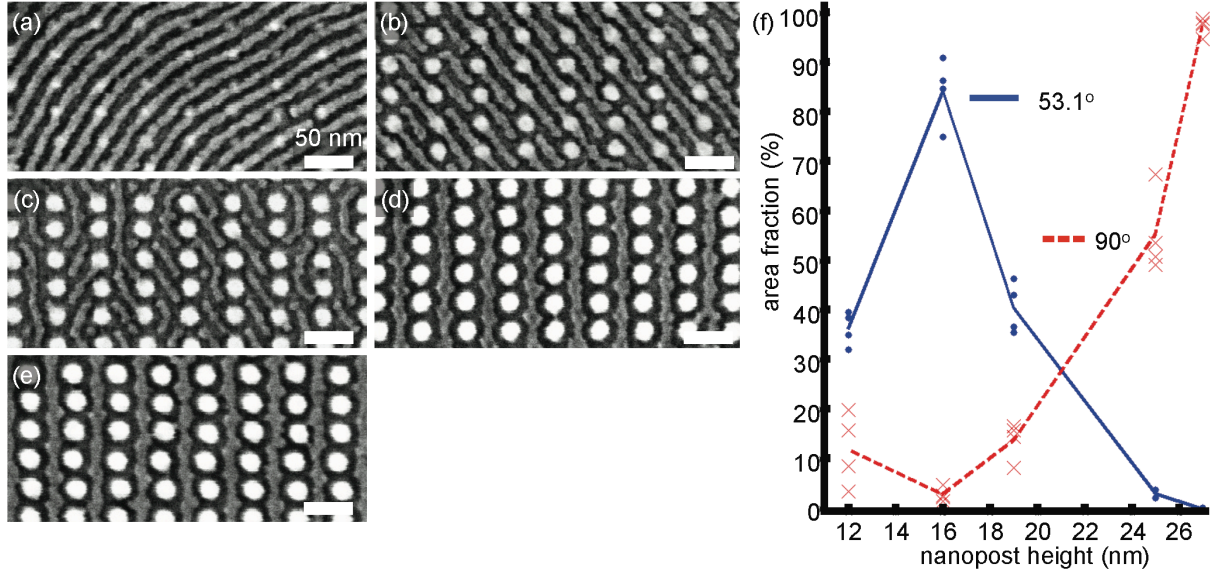
Figure 3. SEM images of PDMS microdomains templated by post arrays with various heights. L_x and L_y of the array was 48 nm and 32 nm respectively. The diameter of posts was 12 nm, and the height of posts was (a) 12 nm (b) 16 nm (c) 19 nm (d) 25 nm (e) 27 nm. Scale bar = 50 nm. (f) the area fractions of the cylinders oriented along the commensurate orientation and the y-axis. Each set of post height data came from a separate sample. (a~e) the samples were slightly overetched, which makes the PDMS cylinders disconnected.

To gain further insight into how PDMS microdomains interact with tall or short posts, we used self-consistent field theory (SCFT) simulation. SCFT has been shown to agree with experimental results, and to predict 3D morphologies of block copolymers.[31-33] In the SCFT simulations, the volume fraction of PDMS $f_{PDMS} = 0.33$, and $\chi N = 14.0$ where χ is the effective Flory-Huggins interaction parameter based on the equilibrium solvent uptake and $N = 69$ is the number of coarse-grained segments corresponding to a Kuhn monomer. For the experimental block copolymer, $\chi = 0.26$ at room temperature and $N = 174$, giving $\chi N = 45.2$. The details of the simulations are included in the Supporting Information. Since the simulation implicity accounts 11

for the solvent by using a lower effective χ and also coarse-grains the polymer by a factor of 2.5 in number of repeat units, the χN used in the model was much lower than the value based on the 0.26 bulk χ parameter and 174 degree of polymerization. Figure 4 shows the simulation result of block copolymer cylinders templated by posts with a range of heights, 12, 19 and 27 nm. The as-spun polymer film in the experiment was 24 nm thick, equivalent to $1.33L_o$. During the solvent annealing process, the polymer film swelled 1.6 times compared with the original film thickness. To simulate templated self-assembly during the solvent annealing process, the film thickness in the model was set as $2.11L_o$ to reflect the swelling of the film by the solvent. As in the experiment, the posts and substrate and the air interface of the film were attractive to the PDMS block, and the model shows PDMS wetting these surfaces.

The 12 nm post ($0.67L_o$) in the simulation led to the formation of a bicontinuous network of PDMS due to the periodic boundary conditions, implying that the cylinders could orient in either direction, as shown in figure 4(a,d,g). This structure is consistent with the experimental observation that the 12 nm posts did not induce long-range order because they were too short to make contact with the PDMS microdomains embedded in the PS matrix. Figure 4(b,e,h) shows the cylinders templated by posts with a height of 19 nm ($1.06L_o$). The PDMS cylinders were in contact with the PDMS-coated posts, and were aligned along the commensurate orientation, with bulges corresponding to the post locations. However, when the height of posts was 27 nm ($1.5L_o$), the cylinders were not connected to the posts even though the posts had a layer of PDMS surrounding them, as shown in figure 4(c,f,i), and the cylinders lay along the larger gaps between the posts, as seen experimentally.

Figure 4(i) also shows why the diameter of posts in the SEM images of Figure 3 appeared different depending on the height of the posts, even though all posts were fabricated with the

same electron dose. A thicker layer of PDMS from the block copolymer surrounded the taller posts, according to the simulations. The oxygen etching preserves the PDMS layer, making the final diameter of the posts larger than the as-fabricated HSQ posts.
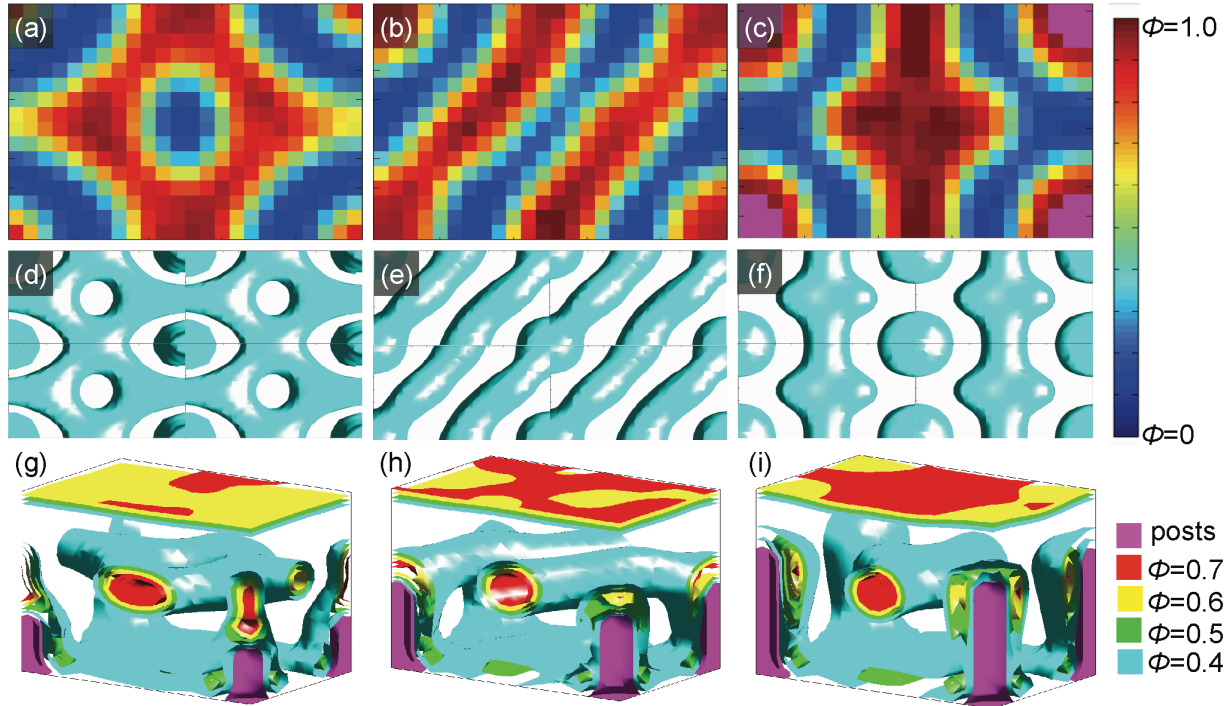

Figure 4. Unit-cell SCFT simulations of templated self-assembly of 16 kg/mol PS-b-PDMS modeled with $\chi N = 14.0$ and $f_{\text{PDMS}} = 0.33$ templated by posts with various heights. (a~c) cut-through cross-section 2D view at height of $1.11L_{\text{o}}$; (d~f) top-down view of 2x2 unit cells; (g~i) 3D view. In terms of L_{o}, the cell thicknesses are $2.11L_{\text{o}}$ corresponding to an evolving solvent annealing thickness of approximately 1.6 times the initial film thickness. The height of posts in terms of L_{o} is (a,d,g) $0.67L_{\text{o}}$ (b,e,h) $1.06L_{\text{o}}$ (c,f,i) $1.50L_{\text{o}}$. These heights correspond to the respective heights in experiment of 12 nm, 19 nm, and 27 nm.

The preceding results suggest that there is an optimum post height (~16 nm, similar to the height of the cylinders above the substrate) and diameter (~11 nm, similar to $L_o/2$ or the diameter of the cylinders) to obtain effective templating. To illustrate the window of post dimensions that provide the best templating, Figure 5 shows the area fraction of cylinders with commensurate orientation as a function of post height and diameter. The smaller posts gave poor templating while the larger diameter and height posts promoted a y-axis orientation, acting analogously to a topographical trench[9]. These results indicate the tolerance of the templating process to variations in post dimensions and provide guidelines for templating lower molecular weight block copolymers or complex structures using size-controlled orientation control within specific areas of the substrate.
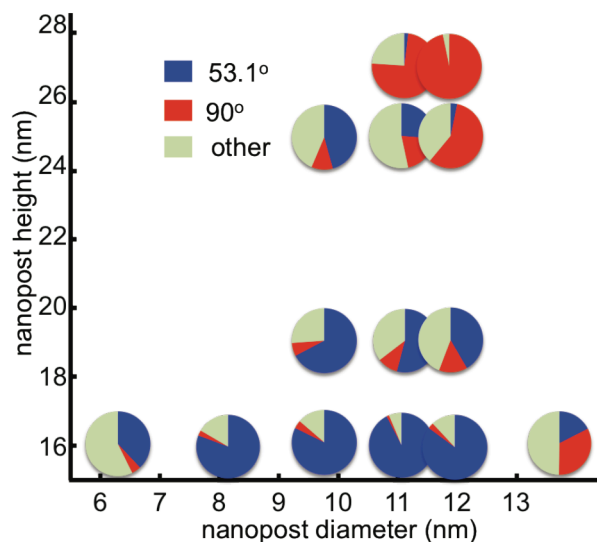

Figure 5. The change of area fraction of the block copolymer cylinders templated by various posts. (a) Pie charts show area fractions of the block copolymer cylinders oriented along the commensurate orientation (53.1°), the y-axis (90°), and other orientations.

Conclusion

This work has shown that a cylindrical morphology PS-*b*-PDMS block copolymer with a period below 20 nm which forms microdomains with a diameter below 10 nm can be registered and oriented in plane using an array of functionalized topographic posts. Posts with a range of diameters and heights were fabricated from a high-contrast resist and a high-contrast development system, and their templating effects were tested. The diameter and the height of posts are major factors determining the interaction between the block copolymer cylinders and the posts and therefore the effectiveness of the templating. The templating is optimized when the post diameter is similar to or smaller than the diameter of the cylindrical microdomains so that the distortion of the microdomains in contact with the posts is minimized, and when the height of the posts is similar to the height of the microdomains above the surface of the substrate. When templated by posts with appropriate diameter and height, the in-plane orientation of the cylinder array is determined by the commensurability between the post lattice and the equilibrium period, analogously to results on a 45.5 kg/mol PS-*b*-PDMS block copolymer with a larger period. In the optimized case the area fraction of the microdomains oriented along the commensurate orientation reached 92%. Short posts were ineffective at templating, while tall or wide posts promoted alignment of the cylinders along the *y*-axis, acting similarly to trenches[9]. Self-consistent field theory modeling illustrated the 3D arrangement of the microdomains and was in good agreement with the observations of post height effect. These findings enable an improved design of sparse topographic templates to direct the assembly of block copolymer patterns with a controlled in-plane orientation and sub-10-nm features. This suggests that templated self-assembly of block copolymers based on sparse topographic templates, formed for example by

interference lithography followed by trimming down and replication by nanoimprint, could be used for fabricating sub-10-nm nanopatterns with high throughput.

Experimental Methods

Poly(styrene-block-dimethylsiloxane) (PS-*b*-PDMS) diblock copolymer was purchased from Polymer Source. The molecular weight of the block copolymer was 16 kg/mol with polydispersity index of 1.08. The in-plane equilibrium spacing (L_o) of the block copolymer cylinders in a thin film after the PS matrix was removed by reactive ion etching was 18 nm. The hydroxyl-terminated PDMS brush (Mn = 0.8kg/mol, PDI ~1.10) was also purchased from Polymer Source. Hydrogen silsesquioxane (HSQ), a negative-tone electron-beam resist, was used for fabricating the topographic templates. 1% HSQ (XR-1521, solids) was purchased from Dow Corning.

HSQ films were spun coated to a thickness of 27 nm, 25 nm, 19 nm, 16 nm, and 12 nm by using spin speeds ranging from 1,000 rpm to 6,000 rpm on 3-inch silicon wafers. The thickness of the HSQ film was determined by ellipsometry. The HSQ coated silicon wafers were cleaved into 2 cm by 2 cm pieces. Single-pixel dots or short dashes (consisting of a short single-pass line) were exposed in a Raith 150 electron-beam lithography tool at 30 kV acceleration voltage. A range of post diameters was achieved from 6.5 nm to 15 nm by varying the electron dose. The samples were developed in a high-contrast developer system as described previously to remove unexposed resist and to reveal the topographic templates[30]. The sample was further treated with O_2/He plasma (50W, 10sec) to remove possible organic residues and to completely convert the HSQ structures into silicon oxide. Then, PDMS brush solution (1% in toluene) was spin coated

on the substrate and thermally treated overnight at 170°C in vacuum. After the thermal treatment, residual brush molecules were removed by rinsing several times with toluene.

0.7 wt% of 16 kg/mol PS-*b*-PDMS dissolved in cyclohexane was spin-coated at 5000 rpm on PDMS brush coated template substrates. The block copolymer films were then exposed to solvent vapors using 1ml of acetone in a 9.3ml volume of glass chamber with a controlled leak until complete evaporation of solvent. The annealing process took approximately 4 hrs. During the solvent annealing, the film swelled up to 1.5 times its original thickness and gradually relaxed as the solvent vapor pressure decreased[28]. To measure the thickness of films during solvent annealing, a Filmetrics F20-UV (Filmeterics, Inc.) instrument was used with a quartz window in the solvent annealing chamber. The annealed BCP films were first treated with a 2 sec, 50W, 10 mTorr CF_4 plasma and then a 12 sec, 50W, 6 mTorr O_2 plasma to remove first the PDMS surface layer and then the PS matrix to leave oxygen-plasma-modified PDMS cylinders on the substrate. The surface morphology was observed using a Raith 150 SEM operated with an acceleration voltage of 10 kV.

Supporting Information Available

Theoretical background to the maximum throughput increase that can be achieved by posts is provided. SEM images of long-range ordered block copolymer patterns templated by dashes are provided. This material is available free of charge *via* the Internet at http://pubs.acs.org.

References

1. Leibler, L. Theory of Microphase Separation in Block Copolymers. *Macromolecules* **1980**, 13, 1602–1617.

2. Bates, F. S.; Fredrickson, G. H. Block Copolymer Thermodynamics: Theory and Experiment. *Annu. Rev. Phys. Chem.* **1990**, 41, 525–557.

3. Lazzari, M.; Lopez-Quintela, M. A. Block Copolymers as a Tool for Nanomaterial Fabrication. *Adv. Mater.* **2003**, 15, 1583–1594.

4. Segalman, R. A.; Yokoyama, H.; Kramer, E. J. Square Packing and Structural Arrangement of ABC Triblock Copolymer Spheres in Thin Films. *Adv. Mater.* **2001**, 13, 1152–1155.

5. Park, M.; Harrison, C.; Chaikin, P. M.; Register, R. A.; Adamson, D. H. Block Copolymer Lithography: Periodic Arrays of ~10^{11} Holes in 1 Square Centimeter. *Science* **1997**, 276, 1401–1404.

6. Segalman, R. A.; Hexemer, A.; Kramer, E. J. Edge Effects on the Order and Freezing of a 2D Array of Block Copolymer Spheres. *Phys. Rev. Lett.* **2003**, 91, 196101.

7. Tang, C. B.; Lennon, E. M.; Fredrickson, G. H.; Kramer, E. J.; Hawker, C. J. Evolution of Block Copolymer Lithography to Highly Ordered Square Arrays. *Science* **2008**, 322, 429–432.

8. Son, J. G.; Hannon, A. F.; Gowtrik, K. W.; Alexander-Katz, A.; Ross, C. A. Hierarchical Nanostructures by Sequential Self-Assembly of Styrene-Dimethylsiloxane Block Copolymers of Different Periods. *Adv. Mater.* **2011**, 23, 634–639.

9. Jung, Y. S.; Chang, J. B.; Verploegen, E.; Berggren, K. K.; Ross, C. A. A Path to Ultranarrow Patterns Using Self-Assembled Lithography. *Nano Lett.* **2010**, 10, 1000–1005.

10. Cheng, J. Y.; Jung, W.; Ross, C.A. Magnetic Nanostructures from Block Copolymer Lithography: Hysteresis, Thermal Stability, and Magnetoresistance. *Phys. Rev. B* **2004**, 70, 064417.

11. Black, C. T. Self-aligned Self-Assembly of Multi-nanowire Silicon Field Effect Transistors. *Appl. Phys. Lett.* **2005**, 87, 163116.

12. Thurn-Albrecht, B.; Schotter, J.; Kastle, G. A.; Emley, N.; Shibauchi, T.; Krusin-Elbaum, L.; Guarini, K.; Black, C. T.; Tuominen, M. T.; Russell, T. P. Ultrahigh-Density Nanowire Arrays Grown in Self-Assembled Diblock Copolymer Templates. *Science* **2000**, 290, 2126–2129.

13. Naito, K.; Hieda, H.; Sakurai, M.; Kamata, Y.; Asakawa, K. 2.5-Inch Disk Patterned Media Prepared by an Artificially Assisted Self-Assembling Method. *IEEE Trans. Magn.* **2002**, 38, 1949–1951.

14. Jung, Y. S.; Jung, W.; Tuller, H. L.; Ross, C. A. Nanowire Conductive Polymer Gas Sensor Patterned Using Self-Assembled Block Copolymer Lithography. *Nano Lett.* **2008**, 8, 3776–3780.

15. Chang, L.; Bao, X.; Bencher, C.; Philip Wong, H. –S. Experimental Demonstration of Aperiodic Patterns of Directed Self-Assembly by Block Copolymer Lithography for Random Logic Circuit Layout. *IEEE IEDM*. **2009**, 33.2.1–33.2.4.

16. Son, J. G.; Bulliard, X.; Kang, H. M.; Nealey, P. F.; Char, K. Surfactant-Assisted Orientation of Thin Diblock Copolymer Films. *Adv. Mater.* **2008**, 20, 3643–3648.

17. Cheng, J. Y.; Rettner, C. T.; Sanders, D. P.; Kim, H. C.; Hinsberg, W. D. Dense Self-Assembly on Sparse Chemical Patterns: Rectifying and Multiplying Lithographic Patterns Using Block Copolymers. *Adv. Mater.* **2008**, 20, 3155–3158.

18. Kim, S. O.; Solak, H. H.; Stoykovich, M. P.; Ferrier, N. J.; de Pablo, J. J.; Nealey, P. F. Epitaxial Self-Assembly of Block Copolymers on Lithographically Defined Nanopatterned Substrates. *Nature* **2003**, 424, 411–414.

19. Ruiz, R.; Kang, H. M.; Detcheverry, F. A.; Dobisz, E.; Kercher, D. S.; Albrecht, T. R.; de Pablo, J. J.; Nealey, P. F. Density Multiplication and Improved Lithography by Directed Block Copolymer Assembly. *Science* **2008**, 321, 936–939.

20. Stoykovich, M. P.; Muller, M.; Kim, S. O.; Solak, H. H.; Edwards, E. W.; de Pablo, J. J.; Nealey, P. F. Directed Assembly of Block Copolymer Blends into Nonregular Device-Oriented Structures. *Science* **2005**, 308, 1442–1446.

21. Cheng, J. Y.; Ross, C. A.; Smith, H. I.; Thomas, E. L. Templated Self-Assembly of Block Copolymers: Top-Down Helps Bottom-up. *Adv. Mater.* **2006**, 18, 2505–2521.

22. Black, C. T.; Bezencenet, O. Nanometer-Scale Pattern Registration and Alignment by Directed Diblock Copolymer Self-Assembly. *IEEE Trans. Nanotechnol.* **2004**, 3, 412–415.

23. Park, S.; Lee, D. H.; Xu, J.; Kim, B.; Hong, S. W.; Jeong, U.; Xu, T.; Russell, T. P. Macroscopic 10-Terabit–per–Square-Inch Arrays from Block Copolymers with Lateral Order. *Science* **2009**, 323, 1030–1033.

24. Bita, I.; Yang, J. K. W.; Jung, Y. S.; Ross, C. A.; Thomas, E. L.; Berggren, K. K. Graphoepitaxy of Self-Assembled Block Copolymers on Two-Dimensional Periodic Patterned Templates. *Science* **2008**, 312, 339–343.

25. Yang, J. K. W.; Jung, Y. S.; Chang, J.; Mickiewicz, R. A; Alexander-Katz, A.; Ross, C. A.; Berggren, K. K. Complex Self-Assembled Patterns Using Sparse Commensurate Templates with Locally Varying Motifs. *Nature Nanotechnol.* **2010**, 5, 256–260.

26. Hirai, T.; Leolukman, M.; Liu, C. C.; Han, E.; Kim, Y. J.; Ishida, Y.; Hayakawa, T.; Kakimoto, M.; Nealey, P. F.; Gopalan, P. One-Step Direct-Patterning Template Utilizing Self-Assembly of POSS-Containing Block Copolymers. *Adv. Mater.* **2009**, 21, 4334–4338.

27. Xu, J.; Hong, S. W.; Gu, W.; Lee, K. Y. Kuo, D. S.; Xiao, S.; Russell, T. P. Fabrication of Silicon Oxide Nanodots with an Areal Density Beyond 1 Teradots inch^{-2}. *Adv. Mater.* **2011**, early view.

28. Son, J. G.; Chang, J.; Berggren, K. K.; Ross, C. A. Assembly of Sub-10-nm Block Copolymer Patterns with Mixed Morphology and Period Using Electron Irradiation and Solvent Annealing. *Nano Lett.* **2011**, 11, 5079–5084.

29. Jung, Y. S.; Ross, C. A. Solvent-Vapor-Induced Tunability of Self-Assembled Block Copolymer Patterns. *Adv. Mater.* **2009**, 21, 2540–2545

30. Yang, Y. J. K.; Berggren, K. K. Using High-Contrast Salty Development of Hydrogen Silsesquioxane for Sub-10-nm Half-pitch Lithography. *J. Vac. Sci. Technol B* **2007**, 25, 2025–2029.

31. Fredrickson, G. H. Self-Consistent Field Theory. In *The Equilibrium Theory of Inhomogeneous Polymers*; Oxford University Press: Oxford, England, 2006; pp 203–276.

32. Alexander-Katz, A.; Fredrickson, G. H. Diblock Copolymer Thin Films: a Field-Theoretic Simulation Study. *Macromolecules* **2007**, 40, 4075–4087.

33. Mickiewicz, R. A.; Yang, J. K. W.; Hannon, A. F.; Jung, Y.; Alexander-Katz, A.; Berggren, K. K.; Ross, C. A. Enhancing the Potential of Block Copolymer Lithography with Polymer Self-Consistent Field Theory Simulations. *Macromolecules* **2010**, 43, 8290–8295.